

na podstawie:  
Lomnitz-Adler J., Automaton models of seismic fracture: Constraints imposed by the magnitude-frequency relation, J. Geophys. Res., 98(B10), 1993

model(e) z Lomnitz-Adler (1993)

#init:  
randomowe wartości h na każdym bloku

#drive:  
wzrost h o określoną wartość na randomowym bloku (random loading)  
#lub  
wzrost h o jednakowe wartości na każdym bloku (homogenous loading)

$\Delta t$  =time\_step

#start lawiny:  
jeśli (model natychmiastowy):  
    jeśli ( $h_0 > h_{\text{graniczne\_startu}}$ ):  
        toppling  
else\_jeśli (model z delay'em):  
    jeśli ( $h_0 > h_{\text{graniczne\_startu}}$ ):  
        append bloku do listy kandydatów

K=len(lista kandydatów)  
dla każdego  $\delta t = \Delta t / K$  # time\_step dla losowania  
dla losowo wybranego bloku z listy\_kandydatów:  
    z prawdopodobieństwem  $\Delta t / \tau$ : #  $\tau$  – skala czasowa dla startu pęknięcia  
        toppling #możliwe >1 w danym time\_stepie

#toppling:

#skończona prędkość propagacji pęknięcia → stosujemy „shell”e

#tzn. w danym kroku bierzemy shell z (najbliższych) sąsiadów bloku pękniętego w poprzednim kroku

dla każdego shellu:

  dla każdego bloku w shellu:

    jeśli ( $h_0 > h_{\text{graniczne\_propagacji}}$ ):

      blok pęka

$h_0 = 0$

    jeśli (model PSD):

      #Partial Stress Drop

      dla każdego z sąsiadów:

$h += v \cdot h_0 / 4$

        #lub ogólniej  $v \cdot h_0 / z$ , z – l. sąsiadów

        #v – zadany ułamek energii przenoszący się do sąsiadów z danego bloku

    else\_jeśli (crack model):

      k=liczba niepękniętych sąsiadów

      jeśli (k):

        dla każdego z niepękniętych sąsiadów:

$h += v \cdot h_0 / k$

boundries:

siatka otoczona jest blokami niepękniętymi

be modeled, at least qualitatively, by means of a nearest-neighbor model.

In the absence of earthquakes the  $h(i, j)$  increase with time at a rate which, when averaged over sufficiently long times, is constant and independent of position. A common assumption is that in the absence of earthquakes, the stress at all points on the fault increases by the same amount. We shall refer to this as the homogenous loading hypothesis.

It is believed that real faults are rough and that their material properties vary over space, and probably over time. Furthermore, any given fault is surrounded by other faults whose earthquakes occur to some extent independently of each other and whose influence on different points of the fault under consideration varies with position. These effects can be included to some extent by incorporating an element of randomness in the temporal and spatial variation of stress on the fault. Models for which this randomness predominates will be referred to as models with random loading: at every time step a site is chosen at random and the stress at this site is increased by a specific amount  $\epsilon$ . As  $\epsilon \rightarrow 0$ , the homogenous loading model is recovered.

With respect to the initiation of rupture, we were interested in studying two features of the nucleation process: the threshold for initiation of fracture and the time scale over which the instability nucleates. It was considered that a certain threshold  $h_t$  exists such that if  $h(i, j) < h_t$ , this particular site is incapable of initiating a fracture, whereas if this value is exceeded fracture can in principle nucleate.

When an earthquake occurs, the stress at broken sites  $h$  drops from the initial value to a lower base value  $h = 0$ . When these sites release their stress, they transfer some to their immediate neighbors and a fraction of it away from the fault. If  $h$  at one of the neighboring sites exceeds a second threshold  $h_p$ , the fracture propagates, this site ruptures, and the process is repeated.

A popular model of seismic instability contends that seismic events are initiated at strongly stressed sites: sites whose local strength exceeds the stress required to propagate the fracture over the fault. We refer to such models as asperity models, and they correspond to  $h_t > h_p$ . Since the fault's material properties are assumed homogeneous, our models differ from many asperity models in the seismological literature, which often assume that asperities are permanent high-strength regions on the fault plane [Das and Kostrov, 1983; Das and Boatwright, 1985; Dmowska and Lovison, 1992]. In our simulations we have also considered the case in which the converse is true, where the stress required to initiate fracture is less than the stress required to propagate it.

Many models of fracture assume that the time scale over which the instability develops is comparable to the time scale of fracture propagation. We refer to these as frictional instability models. Models in which the instability develops slowly over a time scale of days or months have also been considered and will be referred to as rheological instability models. Such models were implemented in the computer by associating a fixed probability of rupture per unit time ( $1/\tau$ ) to each site whose stress exceeds the threshold.  $\tau$  is the time scale of fracture initiation. An example of a rheological model with  $h_t < h_p$  is the one proposed by Lomnitz-Adler [1988].

In the propagation of fracture we shall on the one hand consider crack models, meaning systems in which broken

sites are unable to accumulate stress for the duration of the fracture, and partial stress drop (PSD) models which can [Brune, 1970, 1976]. The crack model corresponds to a dynamic friction force with a very weak velocity dependence. In a partial stress drop model, fractured sites on the fault plane must be able to lock before the seismic event has terminated, implying that the rise time at any one point is very much shorter than the fracture duration so that fracture propagates as a slip pulse.

For some applications, such as reproducing the crack size dependence of the stress singularity at a crack tip, it is convenient to assume that  $h$  is locally conserved over the fault plane [Lomnitz-Adler et al., 1992]. In these cases it is convenient to interpret  $h$  as an energy, say

$$h = a^3 \sigma_{ij} \sigma_{ij} / \mu, \quad (1)$$

where  $a$  is the lattice spacing. When a site with initial energy  $h$  breaks, it transfers only a fraction  $\nu$  of its energy to its neighbors. The fraction  $(1 - \nu)$  can be considered to simulate losses by seismic radiation. We refer to models with  $\nu = 1$  as conservative and with  $\nu < 1$  as nonconservative models. We also note that  $h$  is also lost at the system boundaries, which are totally dissipative.

All possible combinations of these variables were considered, with the exception of instantaneous models whose  $h_t < h_p$ , which are considered to be unphysical (i.e., if  $h_t < h_p$ , the mechanism for initiation must differ from that of propagation), resulting in 40 distinct models. Any crack (PSD) model may be transformed into any other by tuning continuous parameters. For example, if we begin with model 16, by increasing the parameter  $h_t/h_p$  we go to model 15; by decreasing this parameter we go to model 20; by making  $\tau$  tend to zero we obtain model 12; as  $\nu$  tends to one we obtain model 8, and as  $\epsilon$  tends to zero we obtain model 14 (see Figure 1). In this sense we do not really have 40 separate classes of models. Our classification distinguishes between regions of parameter space which present conceptually different seismological models. To clarify this distinction, consider models 15, 16 and 20 which pass from one to the other by varying  $h_t/h_p$  from a value greater than one, to one, to values less than one. If  $h_t/h_p$  we are considering systems in

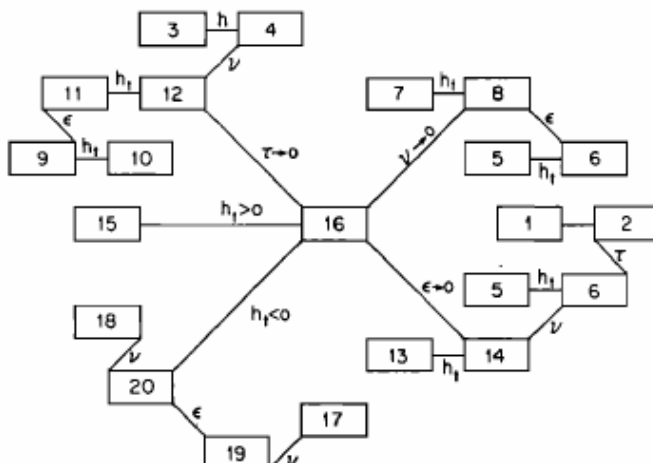


Fig. 1. Illustration of relation between different crack models: any crack model may be obtained from any other by tuning the continuous parameters indicated above the connecting line. A similar figure may be constructed for PSD models.

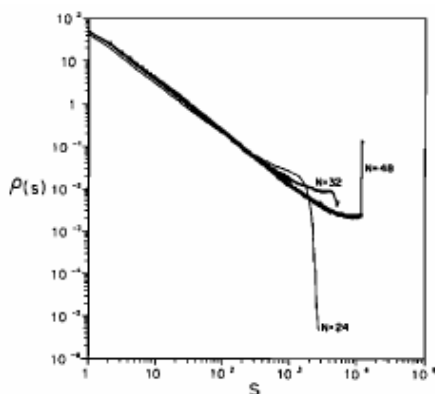


Fig. 9. Scaling behavior of an avalanche model of type III\*. The distribution is bimodal with a power law like behavior ending in a maximum at large avalanche sizes. As the system size is increased, the large-S maximum gains in importance relative to the power law region. Data were obtained from model 22.

## NUMERICAL RESULTS

### Numerical Implementation

In this section we describe explicitly the algorithms used for the different models to evolve in time. We begin by describing the algorithms of fracture propagation, of which there are two, one for PSD and another for crack models. In both cases we define an internal time for the growth of fracture, corresponding to a finite velocity of propagation for the crack front.

1. To implement a finite velocity of fracture propagation, the fracture is grown in successive "shells," which correspond to different internal time steps: The growth sites of the  $n+1$ st shell are the first neighbors of the broken sites of the shell  $n$ th.

2. Within a given shell, consider a growth site. If  $h$  at this site is less than the threshold  $h_p$ , the site does not break and another growth site is tested.

3. If  $h > h_p$ , the site breaks and  $h$  is set to zero. How this energy is redistributed among the neighboring sites depends on the model. If it is a PSD model, then we follow rules "3P":

- 3P. A fixed quantity  $\nu h/z$  is transferred to each of the first neighbors, of which there are  $z = 4$  in all of our simulations.

If it is a crack model we follow rules "3C":

- 3C. We count the number  $k$  of unbroken nearest neighbors and transfer  $\nu h/k$  to each of them. If  $k = 0$ , then the energy contained in the site is lost to the system.

In both cases,  $(1 - \nu)$  is the fraction of the energy lost to the system in any individual rupture.

4. Once a shell has been completely tested, we proceed to the next shell. If no fractures occur within a given shell, the fracture terminates.

In all cases the sites which lie immediately outside the lattice boundaries are treated as unbroken sites.

We next describe the loading and initiation of fracture. If loading is homogenous, the system is initiated by assigning to each site a random value of  $h$ . If initiation is instantaneous, the system is allowed to evolve deterministically until the largest energy value reaches  $h_t$ , at which point a fracture begins. If initiation involves a delay, a list is kept of the sites whose energy exceeds  $h_t$ , which are candidates for fracture initiation. Rather than sampling the entire list at every time

step, we opted for a variable time step  $\delta t = \Delta t/K$ , inversely proportional to the number of sites ( $K$ ) whose  $h > h_t$ . At every time step, one site is chosen at random from the list, and this site fractures with probability  $P_r = \Delta t/\tau$ .

If loading is random, then at every time step  $\Delta t$  a site is chosen at random and a fixed amount of energy  $\epsilon$  is added to it, typically  $\epsilon = h_p/4$ . The global loading rate for the entire system is given by  $\epsilon/\Delta t N^2$ , where  $N$  is the linear lattice size. If fracture initiation is instantaneous, then, if the energy of a site exceeds  $h_t$ , fracture begins and propagates according to the algorithms described above. If fracture does not initiate instantaneously, a list is again kept of all of the sites whose  $h > h_t$ . At every time step this list is sampled in a random order. In each case a random number is generated and, if this number is smaller than  $P_r = \Delta t/\tau$ , a fracture is initiated. The number of events in one time step can be greater than one. In all our simulations,  $\Delta t$  was scaled in such a way that the global loading rate is size independent.

For each class of model we varied the parameters  $\tau$ ,  $h_t/h_p$  and  $\nu$  where relevant. We also carried out simulations on  $24 \times 24$ ,  $32 \times 32$ , and  $48 \times 48$  lattices to study finite size effects and in this way to determine the type of the system under consideration. If necessary,  $64 \times 64$  lattices were also considered. Statistics typically were obtained from 100,000 events, although for some systems we took statistics over as many as  $4 \times 10^6$  events. More than 250 distinct simulations were carried out. Whenever possible we have tried to understand the results of our trial calculation from alternative arguments, such as a nucleation theory or a conservation law.

### Discussion of Results

The results of our simulations are summarized in Table 1, the last column of which indicates the type of size-frequency relation generated by the model. For each such model we carried out a number of such simulations, varying the lattice size as well as the dynamical parameters. Some models were able to generate different types of distributions for different ranges of their parameters. Upon varying the parameters of a given system, its avalanche size distribution may change class, from having a distribution of type I to one of type III. It is thus possible to fine tune the parameters to obtain a power law distribution of type II. We do not consider such situations to be of seismological interest because they lack robustness.

**Type III distributions.** The models which generate type III distributions are shown in Table 2. We note that many of these are crack models and that most crack models with random and homogenous loading give similar results. In those cases where they differ, homogenous models seem to result in type III distributions, where random models do not. The ubiquity of type III distributions for crack models can be understood in terms of the following nucleation model:

First, consider the case in which  $\nu = 1$ , and let us interpret the variable  $h_t$  as the energy contained within a volume  $a^3$  centered at site  $(i, j)$ , where  $a$  is the lattice spacing. The lattice average of the energy per site prior to initiation of fracture will be denoted by  $\langle h \rangle$ ,

$$\langle h \rangle = \Sigma h_{ij} / N^2. \quad (5)$$

On this surface we grow a circular crack of radius  $L$  (in units of  $a$ ). The area which is depleted of energy is equal to  $\pi L^2$ ,